

Spectroscopic Linear Dichroism FT-IR Studies of Synthetic Spider Silk

Y. Koc,¹ P.T. Hammond,² B. Lendl,¹ V.G. Gregoriou*³

¹ University of Technology, Vienna, Austria

² Department of Chemical Engineering, Massachusetts Institute of Technology, Cambridge, MA 02139, USA

³ Foundation for Research and Technology-Hellas, Institute of Chemical Engineering and High Temperature Processes (FORTH - ICE/HT), Patras 26500, Greece
E-mail: gregoriou@iceht.forth.gr

Summary: This work deals with the analysis of the orientation behavior of different segments of synthetic spider silk samples containing hard and soft segments. Two different types of spider silk were examined, one with an aliphatic hard segment (hexamethylene-diisocyanate) and an amorphous soft segment (polytetramethylene oxide) (A40) and the other with an aromatic hard segment (4,4'-methylene bisphenyl diisocyanate) and a semicrystalline soft segment (polyethylene oxide-polypropylene oxide- polyethylene oxide) (A143). In order to observe the orientation behavior of the hard and the soft segments it was necessary to define marker bands. While for both samples the chosen marker bands for the hard segments were the same, the marker bands for the soft segments were different. FT-IR spectra were recorded while strain was applied to the material at the same time. Two parameters, the dichroic ratio R and the order Parameter f were used to evaluate the behavior of these materials under conditions of strain. It was found that sample A143 broke at a strain level of 37,5 %, while sample A40 showed a high dynamic range up to a strain level of 307 %.

Keywords: dichroic ratio; FT- IR spectroscopy; orientation behavior; polyurethanes

Introduction

Spider silk is a material gaining more and more importance in the field of material science due to its extraordinary features. Spider silk is one of the toughest engineering materials known to nature, capable of spanning large areas and bringing flying insects to a halt by dissipating kinetic energy without fracturing. The mechanical properties of spider silk are compared with those of several other engineering materials in Table 1.

Table 1. Comparison of the properties of silk to the properties of other engineering materials.

Material	Modulus (GPa)	Tensile Strength (GPa)	Extensibility (%)	Energy to Break (MJ/m ³)
Dragline Silk	10	1.1	27	160
Viscid Silk	0.003	0.5	270	150
Kevlar 49	130	3.6	2.7	25
High-tensile Steel	200	1.5	0.8	6
Synthetic Rubber	0.001	0.05	850	100

Spider Silk Architecture

The hard blocks in spider silk serve as physical crosslinks within the rubber to prevent macroscopic flow behavior; however, the hard blocks can be melted or cleared at high temperatures, so that the polymer may be melt processed, as an ordinary thermoplastic.

The dragline and frame silks of the *Nephila clavipes* spider are both essentially composed of two proteins, termed Spidroin 1 and Spidroin 2, both of which were characterized²⁸ Spidroin 1 is the dominant component in the stronger dragline silk,

and its amino acid composition is presented in Figure 1. This protein may be considered a *multiblock copolymer*, since it contains several glycine(G)-rich “soft” blocks and alanine-rich “hard” blocks within the same polymer chain. The alanine-rich blocks crystallize to form β -sheet crystals, typically 2 x 5 x 7 nm in size, which are imbedded in a flexible glycine-rich matrix. The polyalanine crystallites serve as physical crosslinks reinforcing the flexible matrix, such that the protein forms a *thermoplastic elastomer*. A thermoplastic elastomer is a block copolymer in which each chain contains chemically immiscible blocks or segments that are thermodynamically

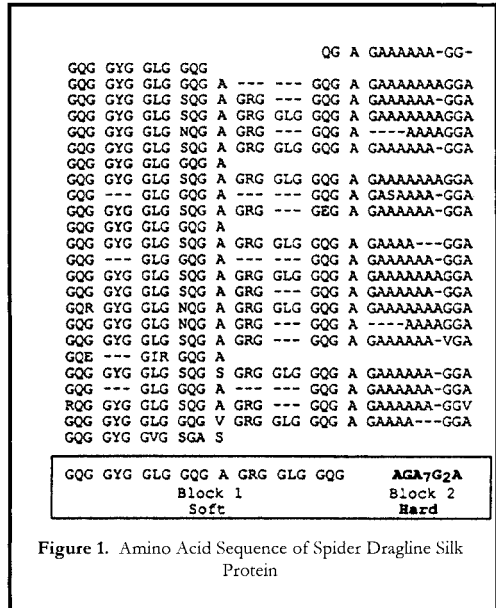


Figure 1. Amino Acid Sequence of Spider Dragline Silk Protein

driven to phase separate. However, the incompatible blocks are covalently linked within the polymer backbone, so the microphase segregate into domains on the length scale of the blocks. Typically, the soft block is above its glass transition temperature, behaving as an amorphous rubber, while the hard block is below its glass transition temperature or melting point, behaving as a rigid reinforcement within the rubbery network. The hard blocks serve as physical crosslinks within the rubber to prevent macroscopic flow behavior; however the hard blocks can be melted or cleared at high temperatures, so that the polymer may be melt processed, as an ordinary thermoplastic.

The task within this work was the approach of finding a material which would mimic the features of synthetic spider silk. Two different samples were chosen which differ from each other in both the hard and soft segments. The hard segment of sample A40 was synthesized on the basis of an aliphatic diisocyanate and a butandiol which should mimic the structure of the polyalanine segments in spider silk. The soft segment was an amorphous polyether which was determined with the help of X-ray diffraction. The hard segment of sample A143 was synthesized on the basis of an aromatic diisocyanate and a butandiol. The soft segment was a segmented semicrystalline ether.

Following figure (2 a b) shows their respective chemical structures.

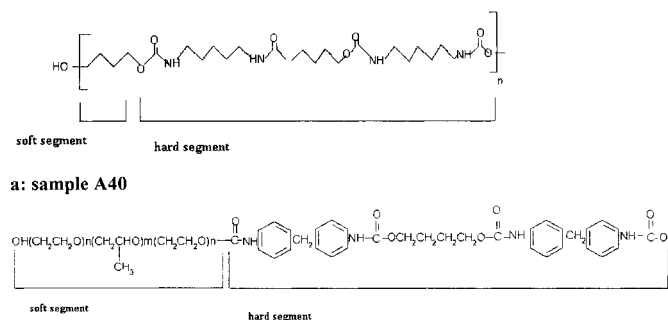


Figure 2: a) Sample A40 with the aliphatic hard segment and the amorphous soft segment. b) Sample A143 with the aromatic hard segment and the semicrystalline soft segment

Stretching experiments were performed in order to observe the orientation behavior of these samples by impinging the polymer films at each step with polarized light, both parallel and perpendicular to the stretch. Both systems behave different from each other during the stretching

procedure. Results are showing differences in behavior between the aliphatic hard segment and the aromatic hard segment. Even the morphology differences in the soft segments show an influence in orientation behavior.

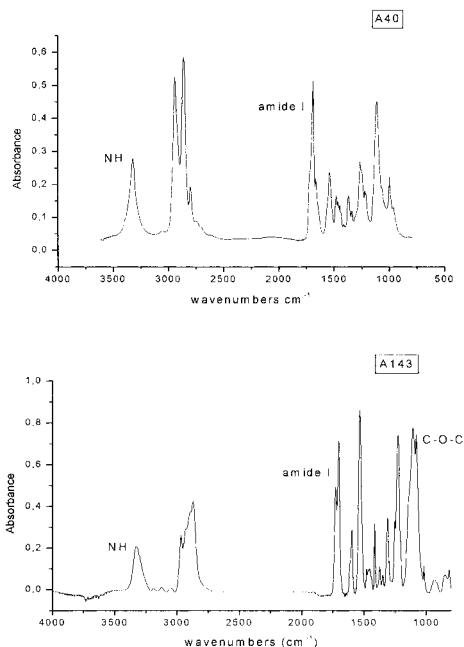


Figure 3: FT-IR spectra of a) Sample A40 and b) sample A143

Table 2. The following marker bands were chosen for samples A40 and A143.

	A40		A143	
	HS	SS	HS	SS
Marker bands	CO(H-bonded)	CO(free)	CO(H-bonded)	C-O-C
			CO(free)	

With the help of curve fitting analysis of the carbonyl bands, the existence of four carbonyl bands can easily be demonstrated. The H-bonded carbonyl bands at 1660cm^{-1} , 1690cm^{-1} and at 1684cm^{-1} and the free carbonyl band at 1714cm^{-1} are present in the spectrum. The bonded carbonyl bands are associated with the behavior of the hard segment while the free carbonyl band demonstrates the behavior of the soft segment.

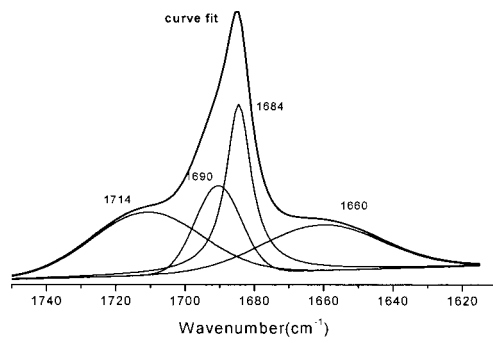


Figure 4: The spectra of A40 have been fit using three Gaussian curves for the bands at 1714, 1690 and 1660 cm^{-1} and a Lorentzian curve for the band at 1684 cm^{-1} in order to obtain the best fit

In the case of A143 the application of curve fitting shows the presence of only two carbonyl bands. The H-bonded carbonyl band at 1701 cm^{-1} and the free carbonyl band at 1728 cm^{-1}

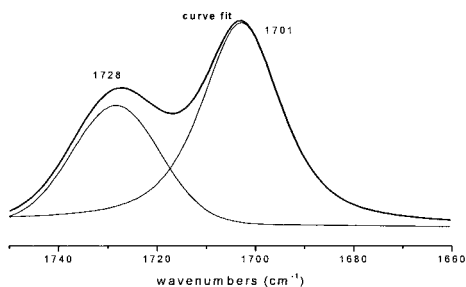


Figure 5: Deconvoluted spectrum of A143

Results and Discussion

The orientation behavior of these two samples is different from each other. While sample A40 only shows orientation in the hard segment, Sample A143 does not show to orient significantly under these conditions.

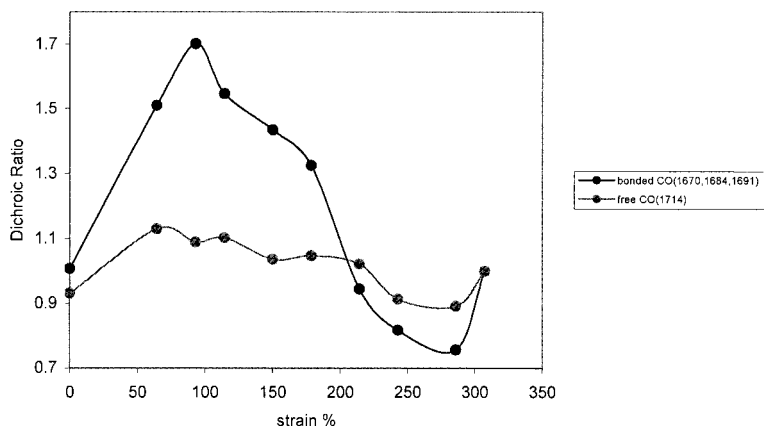


Figure 6: A40: Plot of the dichroic ratio as a function of % strain for the free and the hydrogen bonded carbonyl band

In the case of A40, the bonded carbonyl bands (1660, 1684, 1690) show that there are two different regimes of orientation behavior for the hard segment. At strains up to 97 %, the bonded carbonyl band orients parallel to the stretch direction, suggesting that the hard segment aligns perpendicular to the mechanical field. At strains higher than 97%, the bonded carbonyl band loses its parallel orientation and starts to align in a perpendicular manner. This later orientation is an indication that the hard segment starts aligning parallel with the strain, whereas the free carbonyl does not show a lot of orientation. This orientation behavior leads to the assumption that only the hard segment shows the influence of the stretching procedure. The stretchability of this sample goes up to 307 %, a high number.

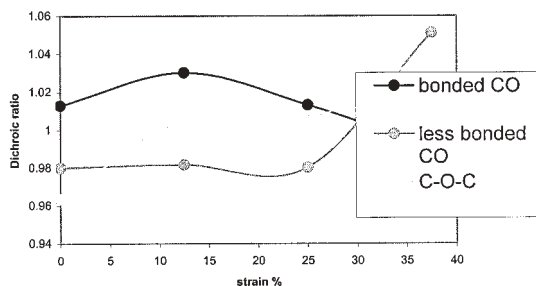


Figure 7: Sample A143 Plot of the dichroic ratio of carbonyl bands and ether band

Three bands are observed in this later stretching experiment. In this case, the ether band is chosen as a representative for the soft segment. The two carbonyl bands are chosen as representatives of the hard segment. The presence of the hard segment is determined by the help of DSC analysis. It was found that the ether band aligns parallel with the strain, suggesting a parallel alignment of the soft segment. In contrast, the carbonyl bands show a behavior opposite to each other within the hard segment. At the beginning, not much orientation is observed but at strains higher than 25 % the bonded carbonyl aligns in a perpendicular direction, suggesting that the actual segment aligns perpendicular. In contrast, the less bonded carbonyl aligns parallel with the strain, suggesting that its segment aligns parallel. This behavior enables the assumption that parts within the hard segment align opposite to each other. Finally, it was observed that this later sample brakes at a strain of 37,5 %, a much lower value than in the case of A40.

Table 3.

	A40	A143
Soft segment	Amorphous	Semicrystalline
Hard segment	Aliphatic	Aromatic
Alignment with strain	HS after a specific strain	SS and a part of HS
stretchability	307 %	38 %

Conclusions

In this work it has been shown that the A40 system is more stretchable than the system A143 and therefore much more likely to mimic the system of spider silk. In addition, the orientation behaviour of both systems was successfully followed by FT-IR linear dichroism techniques

- [1] G. M. Estes, R. W. Seymour, and S. L. Cooper, *Infrared Studies of Segmented Polyurethane Elastomers. II Infrared Dichroism*, University of Wisconsin, **1971**, 22.
- [2] R. Bonart, *X-Ray Investigations Concerning the Physical Structure of Cross- Linking in Segmented Urethane Elastomers*, Engineering Department for Applied Physics, Farbenfabriken BayerAG, Leverkusen
- [3] Weiming Tang, William J. MacKnight, and Shaw L. Hsu, *Segmented Polyurethane Elastomers with Liquid Crystalline Hard Segments. 3. Infrared Spectroscopic Study*, *Macromolecules*, **1995**, 28, 4284
- [4] Hun-Jan Tao, Curtis W. Meuse, Xiaozhen Yang, William J. MacKnight and Shaw L. Hsu., *A Spectroscopic Analysis of Phase Separation Behavior of Polyurethane in Restricted Geometry: Chain Rigidity Effects* , *Macromolecules* **1994**, 27, 7146
- [5] Yue Zhao, Philippe Roche, and Guoxiong Yuan, *Mechanically-Induced Alignment of Mesophases*, *Macromolecules* **1996**, 29 4619
- [6] Fotios Papadimitrakopoulos, Eiji Sawa, and William J. MacKnight, *Investigation of a Monotropic Liquid Crystal Polyurethane Based on Biphenol* , *Macromolecules* **1992**, 25.
- [7] B.R.Nair, V.G. Gregoriou, P.T. Hammond, *FT-IR studies of side chain liquid crystalline thermoplastic elastomers*, *Polymer* **2000**, 41, 2961
- [8] Bindu R. Nair, Marlon A.R. Osbourne, and Paula T. Hammond, *Synthesis and Characterization of New Segmented Copolymers with Side Chain Liquid Crystalline Soft Segments*, *Macromolecules* **2000**, 25, 8749
- [9] Bindu R. Nair, Vasilis G. Gregoriou, and Paula Hammond, *A Study of the Viscoelastic Behavior of Novel Side Chain Crystalline Polyurethanes Using Dynamic Infrared Spectroscopy*, *Journal of Phys. Chem*, **2000**
- [10] Aaron Moment, Ruben Miranda, Paula T. Hammond, *Synthesis of polystyrene-polisiloxane side-chain liquid crystalline block copolymers*, *Macromolecules* **1998**, 573